

Topography, relief, and TRMM-derived rainfall variations along the Himalaya

Bodo Bookhagen^{1,2} and Douglas W. Burbank¹

Received 13 February 2005; accepted 27 March 2006; published 27 April 2006.

[1] Along the southern Himalayan topographic front, the Indian summer monsoon modulates erosive processes and rates. To investigate the influence of topography and relief on rainfall generation and resultant erosion, we processed satellite rainfall amounts for the last 8 years (1998–2005) from the Tropical Rainfall Measurement Mission (TRMM). Based upon a spatial resolution of $\sim 5 \times 5$ km for the Himalaya, we identify (1) the spatial distribution of rainfall and (2) the large-scale relationships between topography, relief, and rainfall locations. Our results show two distinct rainfall maxima along strike in the Himalaya. The first, outer rainfall peak occurs along the southern margin of the Lesser Himalaya within a narrow band of mean elevation (0.9 ± 0.4 km) and mean relief (1.2 ± 0.2 km). The second, discontinuous, inner band typically occurs along the southern flank of the Greater Himalaya (elevation and relief: both 2.1 ± 0.3 km). **Citation:** Bookhagen, B., and D. W. Burbank (2006), Topography, relief, and TRMM-derived rainfall variations along the Himalaya, *Geophys. Res. Lett.*, 33, L08405, doi:10.1029/2006GL026037.

1. Introduction

[2] Across the northern edge of the Indian peninsula, the onset of the Indian summer monsoon (ISM) in early June marks the beginning of the principal rainy season for the Himalaya [e.g., *Fasullo and Webster*, 2003; *Webster and Chou*, 1980]. Every year, the bulk of the annual rainfall occurs between June and September, and thus monsoon rains have vital social and economic consequences [e.g., *Parthasarathy et al.*, 1992]. In addition, rainfall amounts of up to several meters per year result in heavy erosion and flooding along the southern Himalayan front [e.g., *Barnard et al.*, 2001; *Bookhagen et al.*, 2005a; *Gabet et al.*, 2004]. The influence of monsoonal rainfall on the annual Himalayan sediment flux is overwhelming, making the ISM the single, most important factor in understanding Himalayan erosion on long and short timescales [*Bookhagen et al.*, 2005b; *Burbank et al.*, 2003; *Hodges et al.*, 2004; *Thiede et al.*, 2004; *Wobus et al.*, 2003]. Thus, the spatial distribution of ISM rainfall is a critical variable (Figure 1a).

[3] The relationship between rainfall and Himalayan topography, however, remains poorly defined. Due to the remoteness of the Himalaya and lack of reliable rainfall networks, we utilize satellite rainfall estimates from the

Tropical Rainfall Measurement Mission (TRMM). Our analysis of the rainfall data has two components. First, we identify those along-strike zones that are characterized by high average monsoonal rainfall throughout the satellite-measurement period (1998–2005). Second, we explore spatial correlations between rainfall maxima and topographic parameters for ~ 2000 km along strike of the southern Himalayan front to quantify the characteristic elevations and relief at which maximum rainfall occurs. Although the remotely sensed rainfall data cover only 8 years, the intrinsic relation between topographic parameters and rainfall can be used to predict the locus of maximum rainfall for a given Himalayan topography.

2. Methods, Data Sets, and Calibration

[4] We processed raw, orbital data from the Tropical Rainfall Measurement Mission (TRMM) satellite, a multi-sensor satellite that was launched on 27 November 1997 [*Kummerow et al.*, 1998]. The rainfall intensities are primarily derived from two onboard devices with varying spatial resolution: (1) a 5-frequency, passive microwave radiometer (TRMM microwave imager: TMI), with a 10×7 km field of view at 37 GHz, designed after its successful predecessor, the Special Sensor Microwave/Imager (SSM/I) [e.g., *Hollinger*, 1990], and (2) an active precipitation radar (PR) at a frequency of 13.8 GHz with an oval $\sim 4 \times 6$ -km footprint and 250-m vertical resolution. The precipitation radar is the first of its kind in space and permits identification of vertical extent of rainfall structures. Here, we utilize the calibrated, vertically integrated rainfall product for the PR and TMI (following algorithm 2B31, Version 6, accessible at <http://disc.sci.gsfc.nasa.gov/data/datapool/TRMM/index.html>). These data have been projected from their original resolution of 4×6 km and orbital paths to a 5×5 km grid and to an equal-area projection, respectively.

[5] Given its tropical orbit path and ~ 250 -km-wide swaths, the TRMM satellite captures 2 to 4 snapshots of the Himalaya each day. These yield instantaneous rainfall rates calibrated to mm/hr roughly every other day for any given location in the Himalaya. Whereas these measurements are too infrequent to produce a coherent rainfall time series, we integrate over daily measurements for 8 years of satellite data to produce a spatial synthesis. These temporally sparse data prohibit tracking single, short-lived storms, but produce an averaged seasonal rainfall distribution with several hundred instantaneous rainfall measurements at a given location. Because of the non-continuous satellite measurements, monthly or seasonal rainfall amounts are significantly lower than the true rainfall amounts. In order to derive more realistic rainfall amounts, we validated our data against a gauge network in the central Nepalese Himalaya

¹Institute for Crustal Studies, University of California, Santa Barbara, California, USA.

²Now at Geological and Environmental Sciences, Stanford University, Stanford, California, USA.

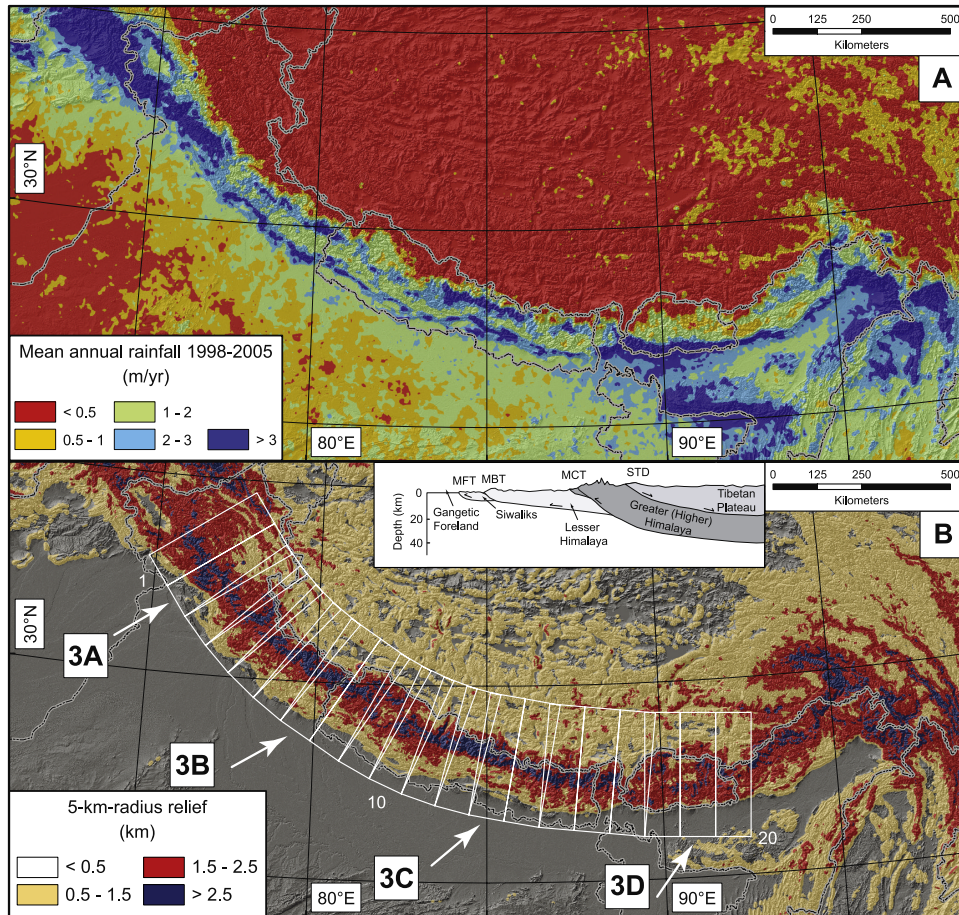


Figure 1. (a) Calibrated TRMM-based monsoon rainfall amounts averaged from January 1998 to December 2005. The data comprises instantaneous rainfall measurement with a spatial resolution of $\sim 5 \times 5$ km. Note the two pronounced rainfall bands in the central Himalaya. (b) 5-km-radius relief calculated from topographic data merged from SRTM V2, DTED, and ASTER-DEM imagery with a spatial resolution of 90 m. Note the high-relief band $\sim 75\text{--}100$ km from the mountain front in the central Himalaya. White polygons indicate the location of 20 swath profiles, of which 4 examples are shown in Figure 3. A simplified N-S geologic profile depicts the major geologic units and faults separating them: Main Frontal Thrust (MFT), Main Boundary Thrust (MBT), Main Central Thrust (MCT).

that represents a continuous rainfall-time series [Barros *et al.*, 2000; Lang and Barros, 2002]. Thus, we utilize the relationship between field measurements and single-cell TRMM-derived rainfall amounts to scale our satellite-derived rainfall amounts (Figure 2). Interestingly, this simple linear fit between TRMM-derived Indian summer monsoon rainfall intensities and absolute rain-gauge amounts yields consistent results. This indicates that, despite non-continuous TRMM-rainfall time series, relative values represent a valid rainfall distribution. Consequently, we apply a constant scaling factor to the satellite data to derive an estimate of the absolute rainfall amount. This relationship, however, holds true only when integrating over satellite rainfall series at least one month long. We suggest this represents a more valid calibration method than comparisons of basin-wide TRMM-derived runoff with river gauges, because a) discharge measurements are more inaccurate than rainfall measurements, b) discharge in the Himalaya is strongly influenced by snowmelt with unknown but likely significant temporal offsets from the precipitation events, and c) very few continuous, reliable discharge measurements are available that account for the

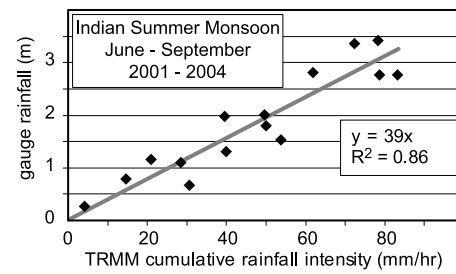


Figure 2. Calibration curve for TRMM-rainfall data utilizing the half-hour rainfall measurement of the central Nepal (Marsyandi) gauge network for the years 2001–2004 [Barros *et al.*, 2000]. Each dot represents the cumulative TRMM-measured rainfall intensity over 4 months (June to September) for one grid cell ($\sim 5 \times 5$ km) vs. the (point-) gauge network measurement. Despite the large differences in spatial and temporal resolution, the data sets agree well. We show only stations that are within 250 m elevation of the corresponding TRMM gridcell.

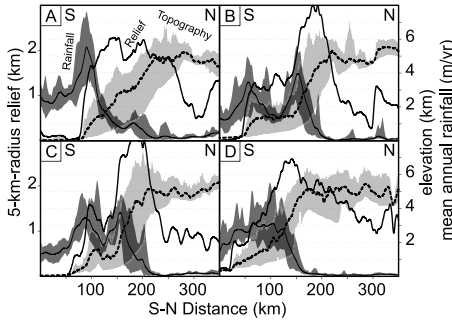


Figure 3. Swath profiles running from south (S) to north (N) (100×350 km) from the (a) northwestern, (b) and (c) central, and (d) eastern Himalaya. Shaded areas denote $\pm 2\sigma$ ranges. Light gray shading denotes topographic and dark gray shading rainfall profiles. Heavy, black line indicates relief. The large increases in relief (Figures 3a, 3b, and 3c) correspond with the southern rainfall maximum. Two rainfall peaks (Figures 3b and 3c) correspond with stepped increases in relief and topography. See Figure 1b for location.

described nocturnal rainfall peak [Barros *et al.*, 2000]. For the purposes of this study, we emphasize that none of the analyses rely on absolute rainfall amounts, but instead we identify rainfall maxima. Despite unavoidable uncertainties from discontinuous time series like TRMM, these data provide the best spatial resolution available today and are much superior to previously published SSM/I data for the Himalaya [Bookhagen *et al.*, 2005a].

[6] We analyzed TRMM rainfall data in the context of topographic data derived from the Shuttle Radar Topographic Mission (SRTM) Version 2 with a spatial resolution of 90 m. The existing holes in the topographic data have been filled with a combination of Digital Terrain Elevation Data (DTED) and digital elevation models derived from Advanced Spaceborne Thermal Emission and Reflection Radiometer (ASTER). This data set has been used to calculate relief with a radius of 5 km.

3. Rainfall and the Indian Summer Monsoon

[7] The Indian summer monsoon (ISM) is part of a larger atmospheric phenomenon, the Intertropical Convergence Zone, that is rooted in seasonal temperature and pressure differences between the northern and southern hemispheres [Gadgil *et al.*, 2003; Webster and Chou, 1980]. In particular, the temperature and resulting pressure gradient between the elevated Tibetan Plateau and surrounding oceans draw moisture from the Bay of Bengal and transport it northwestward. After the onset of the ISM, latent-heat release significantly contributes to maintaining the temperature gradient. When these humid air masses collide with orographic barriers, heavy convection is initiated that leads to high rainfall amounts in the eastern and central Himalaya (Figure 1a) [Barros *et al.*, 2000; Bookhagen *et al.*, 2005a]. In the western Himalaya, rainfall distributions respond to both monsoon moisture from the Bay of Bengal and moisture-bearing westerly winds [Bookhagen *et al.*, 2005a; Hatwar *et al.*, 2005]. Previous studies have revealed two general Himalayan rainfall gradients: (1) an east-west

gradient with higher rainfall occurring closer to the major moisture source, the Bay of Bengal (Figure 1), and (2) a strong north-south gradient across the range from its rain-drenched southern flank to the semi-arid Tibetan Plateau [e.g., Anders *et al.*, 2006; Barros *et al.*, 2000; Bookhagen *et al.*, 2005b; Parthasarathy *et al.*, 1992]. This north-south gradient is a generalized consequence of orographic rainfall [e.g., Barros and Lattenmaier, 1994; Bookhagen *et al.*, 2005a; Roe, 2005], whereby rising topography in the face of prevailing winds causes mechanical lifting of humid air, cooling of the air column, condensation, and precipitation.

[8] The topographic characteristics that modulate orographic rainfall in the Himalaya have not been previously identified. Improved knowledge of why rainfall becomes spatially focused would be valuable, because the location of enhanced rainfall may circumscribe regions affected by high erosion. Thus, developing a conceptual relationship between topography and peak rainfall will aid in understanding how mountain belts erode [e.g., Bookhagen *et al.*, 2005b; Burbank *et al.*, 2003; Thiede *et al.*, 2004; Wobus *et al.*, 2003].

4. Results and Discussion

[9] The new high-resolution TRMM data reveal some striking characteristics of Himalayan rainfall. Whereas significant attention has been focused in the past on the high rainfall that occurs near the toe of the Greater Himalaya [Burbank *et al.*, 2003], as also imaged here, our new data show that an even more continuous band of high rainfall stretches along the southern edge of the Lesser Himalaya near their junction with the Indo-Gangetic foreland basin (Figure 1a). Clearly, heavy rainfall appears to be induced by the first significant topography that is encountered by moist air masses sweeping toward the Himalaya [Haselton, 1998]. The specific controls exerted by the topography, however, remain poorly known.

[10] In order to quantify more precise relationships between topography and rainfall, we analyzed 20 100-km-wide and 350-km-long swath profiles (Figure 1b). At each point in the orogen-perpendicular direction along the swath, we averaged orogen-parallel data for rainfall, elevation, and relief within a 5-km-radius window (Figure 3). (The entire profile set is available in the auxiliary material¹.) When we synthesize data from all swaths, several key characteristics of the rainfall-topographic data emerge. First, zones of highest rainfall are offset a few to 10s of km south of either the highest topography or relief (Figure 3). Second, along the southern margin of the Himalaya, the frontal band of high rainfall occurs at a mean elevation of 0.9 ± 0.4 km and a relief of 1.2 ± 0.2 km (Figures 4a and 4b). Given the 5×5 km resolution of the TRMM data, we calculate the mean (cross-swath) elevation or relief within a range of 5 km up and down slope of the peak rainfall. This initial orographic barrier results from southward thrusting of the Lesser Himalaya over the northernmost, proximal edge of the Himalayan foreland basin. Although this thrusting began at least 10 Ma [Meigs *et al.*, 1995], the Lesser Himalayan rocks remain relatively high standing because deformation

¹Auxiliary material is available at <ftp://ftp.agu.org/pend/g1/2006gl026037>.

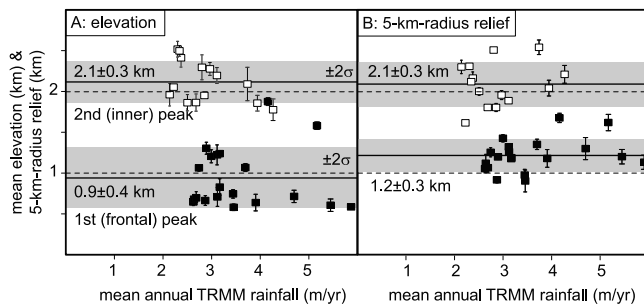


Figure 4. Monsoon rainfall, elevation, and relief from each swath along strike of the Himalaya for ~ 2000 km (Figure 1b). Rainfall values above 3.5 m/yr correspond to the northwestern and eastern parts of the Himalaya. (a) Local maximal rainfall versus mean elevation within 5 km of the maxima. (b) Local maximal rainfall versus relief. Despite 2 -fold rainfall variations along strike, the maximum rainfall occurs within a narrow band of elevation and relief. The inner band of high rainfall is most prominent in the central Himalaya.

is ongoing and these rocks are more resistant to erosion than the Cenozoic strata in the foreland. Third, west of $\sim 88^\circ\text{E}$ in the Sikkim Himalaya (to the west of Bhutan), a second, intermittent, inner band of high rainfall occurs on the upwind side of the range at an elevation of 2.1 ± 0.3 km and an equivalent amount of relief (2.1 km). This band stretches for ~ 1000 km to the Sutlej Valley at $\sim 78^\circ\text{E}$ (Figures 4a and 4b). The location of this rainfall maxima is controlled by topography near the boundary of the Lesser and Greater Himalaya, where it lies ~ 3 km below the highest mean elevation and $\sim 5\text{--}6$ km below the highest Himalayan peaks.

[11] There exist two regions with somewhat contrasting topography and relief distribution that mimic the existing rainfall pattern (Figures 1a and 1b). First, the eastern ($88\text{--}93^\circ\text{E}$) and parts of the northwestern Himalaya ($74\text{--}76^\circ\text{E}$) are characterized by a continuous, rapid change in relief, but by a mean topographic profile that only gradually rises to elevations >4 km (Figures 3a and 3d). These zones of abrupt, sustained increases in relief appear to wring moisture out of monsoon storms. Second, most of the central Himalaya between 78° and 88°E is characterized by two zones of rapidly increasing relief and steps in the topographic profile (Figures 3b and 3c). The first occurs along the leading edge of the Lesser Himalaya and the second occurs near the toe of the Greater Himalaya [e.g., *Gabet et al.*, 2004; *Wobus et al.*, 2003]. As monsoon storms first impinge on the Himalaya, high rainfall occurs as mean relief abruptly rises $1\text{--}1.4$ km above the foreland. The massive topographic front of the Greater Himalaya drives an even larger, abrupt increase in relief of $1.8\text{--}2.4$ km that focuses the second band of heavy rainfall. Generally, regions without the inner rainfall band have steeper relief and larger rainfall amounts at the range front (Figure 1a).

5. Conclusion

[12] Nearly a decade of rainfall data from the Tropical Rainfall Measurement Mission (TRMM) rainfall provides

an unprecedented overview of Himalayan monsoonal precipitation at a high spatial resolution. The data show two discrete bands of high rainfall that stretch along the length of the Himalaya. Although the frontal band is remarkably continuous, the inner band at the toe of the Greater Himalaya is less so. When combined with 90-m digital topography, clear relationships emerge between topographic characteristics and the zones where rainfall maxima occur. These occur in the frontal regions along the entire Himalaya at an average elevation of ~ 0.95 km or a mean relief of ~ 1.2 km. In addition, the central Himalaya are characterized by an inner rainfall belt that occurs at an average ~ 2.1 km elevation or ~ 2 km mean relief. However, the eastern and northwestern regions do not show this inner rainfall belt because topography does not rise in a two-step pattern and high relief appears closer to the mountain front. To the extent that erosion is coupled to rainfall, these bands of high rainfall should modulate erosion. We view relief and relief changes as a surrogate for generalized topographic steepness that can be used as a first-order parameter to identify focused rainfall in mountain belts influenced by monsoonal climates. This, in turn, demonstrates that locations of high, present-day relief most likely received the maximum rainfall amount during past, intensified monsoon phases with similar relief distribution [e.g., *Bookhagen et al.*, 2005b; *Pratt et al.*, 2002].

[13] **Acknowledgments.** The data used in this study were acquired as part of the Tropical Rainfall Measuring Mission (TRMM) sponsored by the Japan National Space Development Agency (NASDA) and the US National Aeronautics and Space Administration (NASA). This work was supported with grants from NASA (NAG5-13758) and NSF (EAR 9909647). We thank R. C. Thiede for comments and C. Wobus and an anonymous reviewer for constructive reviews.

References

- Anders, A. M., et al. (2006), Spatial patterns of precipitation and topography in the Himalaya, *Geol. Soc. Am. Spec. Pap.*, 398, in press.
- Barnard, P. L. (2001), Natural and human-induced landsliding in the Garhwal Himalaya of northern India, *Geomorphology*, 40, 21–35.
- Barros, A. P., and D. P. Lattenmaier (1994), Dynamic modeling of orographically induced precipitation, *Rev. Geophys.*, 32, 265–284.
- Barros, A. P., M. Joshi, J. Putkonen, and D. W. Burbank (2000), A study of the 1999 monsoon rainfall in a mountainous region in central Nepal using TRMM products and rain gauge observations, *Geophys. Res. Lett.*, 27, 3683–3686.
- Bookhagen, B., et al. (2005a), Abnormal monsoon years and their control on erosion and sediment flux in the high, arid northwest Himalaya, *Earth Planet. Sci. Lett.*, 231, 131–146.
- Bookhagen, B., et al. (2005b), Late Quaternary intensified monsoon phases control landscape evolution in the northwest Himalaya, *Geology*, 33, 149–152.
- Burbank, D. W., et al. (2003), Decoupling of erosion and precipitation in the Himalayas, *Nature*, 426, 652–655.
- Fasullo, J., and P. J. Webster (2003), A hydrological definition of Indian monsoon onset and withdrawal, *J. Clim.*, 16, 3200–3211.
- Gabet, E. J., et al. (2004), Climatic controls on hillslope angle and relief in the Himalayas, *Geology*, 32, 629–632.
- Gadgil, S., et al. (2003), The Indian monsoon and its variability precipitation fluctuations in the Nepal Himalaya and its vicinity and relationship with some large scale climatological parameters, *Annu. Rev. Earth Planet. Sci.*, 31, 429–467.
- Haselton, K. R. (1998), Spatial distribution of orographic rainfall in the Himalayan Front and the western Tianshan from satellite data, *Eos Trans. AGU*, 79(46), Fall. Meet. Suppl., Abstract H31D-08.
- Hatwar, H. R., et al. (2005), Prediction of western disturbances and associated weather over western Himalayas, *Current Sci.*, 88, 913–920.
- Hodges, K. V., et al. (2004), Quaternary deformation, river steepening, and heavy precipitation at the front of the higher Himalayan ranges, *Earth Planet. Sci. Lett.*, 220, 379–389.
- Hollinger, J. P. (1990), Special issue on the Defense Meteorological Satellite Program (DMSP)—Calibration and validation of the Special Sensor

- Microwave Imager (SSM/I), *IEEE Trans. Geosci. Remote Sensing*, 28, 779–780.
- Kummerow, C., et al. (1998), The Tropical Rainfall Measuring Mission (TRMM) sensor package, *J. Atmos. Oceanic Technol.*, 15, 809–817.
- Lang, T. J., and A. P. Barros (2002), An investigation of the onsets of the 1999 and 2000 monsoons in central Nepal, *Mon. Weather Rev.*, 130, 1299–1316.
- Meigs, A. J., et al. (1995), Middle-Late Miocene (greater-than-10 Ma) formation of the Main Boundary thrust in the western Himalaya, *Geology*, 23, 423–426.
- Parthasarathy, B., et al. (1992), Indian-summer monsoon rainfall indexes—1871–1990, *Meteorol. Mag.*, 121, 174–186.
- Pratt, B., et al. (2002), Impulsive alluviation during early Holocene strengthened monsoons, central Nepal Himalaya, *Geology*, 30, 911–914.
- Roe, G. H. (2005), Orographic precipitation, *Annu. Rev. Earth Planet. Sci.*, 33, 645–671.
- Thiede, R. C., et al. (2004), Climatic control on rapid exhumation along the Southern Himalayan Front, *Earth Planet. Sci. Lett.*, 222, 791–806.
- Webster, P. J., and L. C. Chou (1980), Seasonal structure of a simple monsoon system, *Atmos. Sci.*, 37, 354–367.
- Wobus, C. W., et al. (2003), Has focused denudation sustained active thrusting at the Himalayan topographic front?, *Geology*, 31, 861–864.

B. Bookhagen, Geological and Environmental Sciences, Stanford University, Stanford, CA 94305, USA. (bodo@pangea.stanford.edu)

D. W. Burbank, Institute for Crustal Studies, University of California, Santa Barbara, CA 93106, USA.